Desalination and Water Treatment
www.deswater.com
doi: 10.1080/19443994.2015.1027959

57 (2016) 9247–9262
April

Taylor & Francis
Taylor & Francis Group

Comparative study of chitin and chitosan beads for the adsorption of hazardous anionic azo dye Congo Red from wastewater

Nirav P. Raval[a], Prapti U. Shah[a], Divya G. Ladha[b], Poonam M. Wadhwani[b], Nisha K. Shah[a,b,*]

[a]*Department of Environmental Science, School of Sciences, Gujarat University, Ahmedabad 380 009, Gujarat, India, Tel. +91 9904721558; email: nirav.raval90@gmail.com (N.P. Raval), Tel. +91 9558825191; email: prapti.shah1126@gmail.com (P.U. Shah), Tel. +91 9825312095, +079 26305037; email: nishchem2004@yahoo.co.in (N.K. Shah)*
[b]*Department of Chemistry, School of Sciences, Gujarat University, Ahmedabad 380 009, Gujarat, India, Tel. +91 9712952953; email: divya.ladha@gmail.com (D.G. Ladha), Tel. +91 8460519967; email: poonam270888@gmail.com (P.M. Wadhwani)*

Received 13 September 2014; Accepted 3 March 2015

ABSTRACT

Chitin (CH) and chitosan (CTS) beads used and compared for the adsorption of Congo Red (CR), an anionic azo dye, are reported in the present work. Initially, the adsorbents were prepared and characterized by scanning electron microscopy (SEM) and Fourier transform infrared (FT-IR) analysis. SEM images showed the heterogeneous and porous structure of the beads and FT-IR results confirm the presence of –OH, $–NH_2$, and–$NHCOCH_3$ groups which are responsible for the adsorption of CR. Further, batch studies were conducted to evaluate the adsorption capacity of CH and CTS beads and the effects of the parameters like pH, adsorbate concentration, contact time, and dosage of adsorbents on adsorption were investigated. From the analysis, it was observed that the amount of CR adsorbed on both the adsorbents increases with increasing initial dye concentration and decreasing pH. The adsorption isotherms were analyzed using the Langmuir and Freundlich isotherms. The Langmuir isotherm was the best-fit adsorption isotherm model for the experimental data obtained from the nonlinear chi-square statistic test. Further, the pseudo-first-order and second-order kinetic models were used to describe the kinetic data, and the rate constants were evaluated. The dynamical data fit well with the second-order kinetic model. The results indicate that CH and CTS beads could be employed as low-cost material for the adsorption of CR from wastewater.

Keywords: Chitin beads; Chitosan beads; Congo Red; Adsorption isotherms; Kinetics; Error analysis

1. Introduction

Textile industry is one of the largest generators of the contaminated effluents, which mainly arise from dyeing and finishing processes [1]. These dyeing effluents have significant characteristics such as wide range of pH, large amount of suspended solids, high oxygen demand, stability to light, heat, and oxidizing agents, and resistance to biodegradation [2]. Thus, discharge of these highly colored waste effluents without

*Corresponding author.

This version has been corrected. Please see Erratum (http://dx.doi.org/10.1080/19443994.2015.1040629).

1944-3994/1944-3986 © 2015 Balaban Desalination Publications. All rights reserved.

proper treatment is not only esthetically displacing but it also impedes light penetration, and thereby it affects the various biological processes within the stream [3,4]. Approximately half of all dyes are azo dyes, making them the largest group of synthetic colorants used in textile industries [5].

Azo dyes are complex aromatic compounds with significant structural diversity and are of great environmental concern because the reductive cleavage of azo linkages is responsible for the formation of amines, which are classified as toxic and carcinogenic [6].Congo Red (CR) [1-naphthalene sulfonic acid, 3,3′-(4,4′-biphenylenebis (azo)) bis (4-amino-) disodium salt] is the most commonly used benzidine-based azo dye. It is usually found in the effluents discharged from textile, paper, printing, and leather industries. It has a complex chemical structure and high solubility in aqueous solution. It is metabolized to benzidine, a known human carcinogen, and exposure to this dye can cause allergic responses [7–9]. Due to all these properties and toxic nature, CR was selected as a model anionic dye in this study.

The traditional techniques applied for the treatment of dyeing effluent are: adsorption [10], coagulation and flocculation [11], oxidation [12], ozonation [13], reverse osmosis [14], membrane filtration [15], electrochemical processes [16], and biological degradation [17]. The application of conventional physicochemical methods has been restricted due to high-energy consumption and expensive chemicals. In addition, these methods generate large amount of toxic sludge, which also creates disposal problem [18]. The biological wastewater treatment techniques are also not effective in the treatment of dye-containing effluent because of the low biodegradability of dyes.

Adsorption has become one of the most economical, effective, and widely used treatment techniques for the removal of dyes from aqueous solution [19]. Basically, adsorption is a mass transfer process by which substance is transferred from the liquid phase to the surface of a solid and gets bound by physical or chemical interactions [20]. Adsorption on activated carbon has been found to be an effective process for the removal of dyes from effluent, but it is too expensive and both regeneration and disposal of the used carbon is often very difficult. Thus, it is a continuing need to identify and develop easily available, economically viable, and highly effective adsorbent for efficient and facile removal process.

In recent time, use of biopolymers is increasing for the removal of dye from wastewater. Biopolymers are high molecular weight compounds synthesized by living organisms. Since they are polymers, they contain monomeric units that are covalently bonded to large structures. Because of this, biopolymers can be used as adsorbents for the efficient removal of hazardous dyes. Chitin (CH) and chitosan (CTS) are considerably versatile and promising biopolymers. CH (Poly [β-(1 → 4)-2-acetamido-2-deoxy-β-D-glucopyranose]), a polymer of N-acetyl-D-glucosamine, is the second most ubiquitous natural polysaccharide after cellulose on earth and is widely distributed in nature, especially in the exoskeletons of marine invertebrates such as shrimps, crabs, prawns, and lobsters. Its main derivative, CTS (Poly [β-(1 → 4)-2-amino-2-deoxy-β-D-glucopyranose]), hetero-polysaccharide of D-glucosamine and N-acetyl-D-glucosamine residues, is obtained by the alkaline deacetylation of CH [21]. Both these biopolymers exhibits a high adsorption capacity towards dyes due to their multiple functional groups, biocompatibility, biodegradability, non-toxicity, and adsorption properties [22]. CTS and cross-linked CTS beads have been used by many researchers to remove various anionic dyes [23,24], cationic dyes [25], and reactive dyes [26,27] from water and wastewater. Recently, a review paper has also been published related to the application of CTS and its derivatives as adsorbents for dye removal from water and wastewater [28].

Thus, the main objective of this study is to adsorb CR dye from wastewater by preparing and characterizing beads from CH and CTS biopolymers, as well as to compare their adsorption capacity towards CR. This study reports, for the first time, CH beads as a low-cost adsorbent for the adsorption of CR.

2. Experimental

2.1. Materials and methods

CH and CTS powder used in this work were purchased from ACS Chemicals Pvt. Ltd. and used as such without further purification. The molecular structures of CH and CTS are shown in Fig. 1(a) and (b). Analytical grade reagents and double-distilled water were utilized unless otherwise specified. CR dye was purchased from the ACS Chemicals Pvt. Ltd. which was dried in an oven before use. Some important chemical properties of the dye are noted in Table 1. The molecular structure of CR is shown in Fig. 1(c). A stock solution (1,000 mg/L) of CR was prepared by dissolving an appropriate amount of dye in deionized water, which was diluted to desired concentrations of 35, 70, 105, and 140 mg/L.

2.2. Preparation of adsorbents

CH solution was prepared by dissolving CH powder in N, N dimethylacetamide/5% Lithium

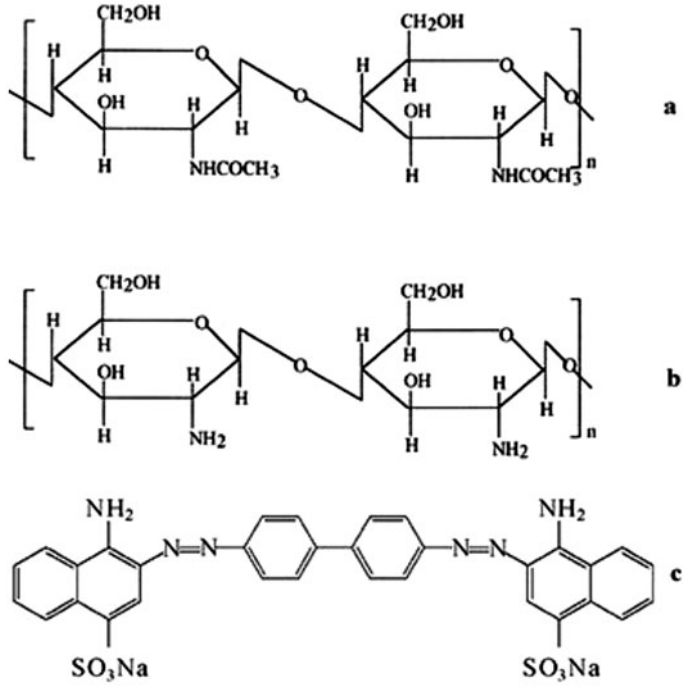

Fig. 1. Molecular structures of CH (a), CTS (b), and CR (c).

Table 1
Physicochemical properties of the dye CR

Parameters	Value
Synonymous	Cotton red, C.I. 22,120
IUPAC name	1-naphthalene sulfonic acid, 3, 3′- (4, 4′-biphenylenebis (azo)) bis (4-amino-) disodium salt
Molecular weight	696.68
Molecular formula	$C_{32}H_{22}N_6Na_2O_6S_2$
Solubility in water	Soluble

Chloride (LiCl) solvent system. Beads were prepared by dropping CH solution into 100 mL of non-solvent coagulant, ethanol, and were left in it for 24 h to remove remaining residual solvent from the beads. Thus, after 24 h, it would give spherical-shaped CH beads [29].

CTS powder was dissolved in 1% (v/v) acetic acid solution to produce a viscous solution with 1% (w/v) CTS. This viscous CTS solution was added dropwise into 100 mL of 5% (w/v) sodium tripolyphosphate (STPP) solution, which neutralized the acetic acid within the CTS gel and thereby coagulated this gel to spherical uniform beads [30].

The CH and CTS beads prepared were filtered, rinsed several times with distilled water, and dried under vacuum. The dried adsorbents were ground to fine powder for further study.

2.3. Instrumentation

The surface morphology of dried CH and CTS beads both before and after CR adsorption were studied using scanning electron microscopy (SEM) (Carl-Zeiss, 40) after coating the beads with gold by electrodeposition under high vacuum. Similarly, the infrared spectra of both the adsorbents under different conditions were characterized using Fourier transform infrared (FT-IR) spectrophotometer (Shimadzu-8400 S) with a KBr pellet. The elemental composition of adsorbents in weight percentage unit was measured using energy dispersive X-ray spectrometer (EDX).

A double beam UV–vis spectrophotometer (Evolution 260 BIO UV–vis. spectrophotometer) was employed to determine the unknown concentration of

CR solutions. The unknown dye concentrations were estimated by interpreting the absorbance with standard calibration curve at (λ_{max}) 497 nm. The aqueous pH measurements were carried out using Equip-Tronics pH meter (Digital pH meter Model No.: EQ-615).

2.4. Batch adsorption studies

Batch adsorption experiments were carried out with the CH and CTS beads for the removal of CR from its aqueous solutions. For each batch, 100 mL of CR solution with varying concentration, pH, and amount of adsorbent were taken in 250 mL beaker. The solution was further stirred at 120 rpm using a magnetic stirrer at room temperature. After regular time intervals, the adsorbents were separated by filtration through glass wool. The absorbance of the filtrate was estimated to determine the residual CR concentration using a UV–vis spectrophotometer at a λ_{max} 497 nm. The experiments were done by varying the concentration of dye solution (35, 70, 105, and 140 mg/L); amount of adsorbents (10–100 mg/100 mL); contact time (1–120 min), and pH values (2.0–9.0) at regular time intervals. The removal percentage ($R\%$) of CR was calculated by following expression:

$$R\% = \frac{(C_0 - C_e)}{C_0} \times 100\% \quad (1)$$

The amount of CR adsorbed (mg/g) was calculated based on a following mass balance equation.

$$q_e = \frac{(C_0 - C_e)V}{W} \quad (2)$$

where q_e (in mg/g) represents the equilibrium adsorption capacity per gram (dry weight) of the adsorbent; C_0 (in mg/L) is the initial concentration of CR in the solution; C_e (in mg/L) is the equilibrium concentration of CR in the solution; V (in mL) is the volume of the solution; and W (in mg) is the dry weight of CH and CTS beads.

3. Results and discussion

3.1. SEM–EDX

SEM investigations at 10.00 K× magnifications were carried out to study the morphological features and surface characteristics of both the adsorbents before and after CR adsorption, and results are illustrated in Fig. 2[A](a)–(d). It is observed from Fig. 2[A](a) that the surface of the CH beads before CR adsorption consists of polymeric network with irregular pores, which becomes flat, smooth, and non-porous after dye adsorption as shown in Fig. 2[A](b). While from Fig. 2[A](c), it is observed that CTS beads have very rough surface which becomes continuous and smooth after dye adsorption because of the monolayer coverage of the dye molecules on the entire surface of the CTS beads which is observed in Fig. 2[A](d). The EDX analysis spectra of CH (a) and CTS (b) beads were shown in Fig. 2[B]. From the EDX spectra, it is clearly observed that the CH and CTS beads consist of mainly carbon (C), nitrogen (N), and oxygen (O). Further, the CTS beads also consist of phosphorus (P) and sodium (Na) in 5.08 and 0.83 wt.%, respectively.

3.2. FT-IR

The surface groups of the adsorbents, which are responsible for the dye adsorption can be examined and identified using FT-IR data. The presence of characteristic peaks and active sites of the adsorbents were confirmed with the FT-IR spectra.

As observed in Fig. 3[A](a) and (b), the strong bands at 3,481.27 and 3,431.13 cm^{-1} were attributed to stretching vibration of –OH groups present on the CH and CTS beads, respectively, and bands at 3,274.90 and 3,089.75 cm^{-1} belong to asymmetric and symmetric stretching vibration of –NH from $–NHCOCH_3$ groups present on the CH beads. In Fig. 3[A](a) and (b), the bands observed at 2,933.53 and 2,920.03 cm^{-1}, respectively, were assigned to $–CH_3$ stretching vibration which are supported by the existence of absorption at 1,377.08 cm^{-1}, characteristic for the bending vibration of $–CH_3$. The spectrum of CTS beads Fig. 3[B](c). showed a sharp peak at 1,554.52 cm^{-1}, indicating the ionic interaction between NH^{3+} groups of CTS and PO_4^{-3} groups of sodium tripolyphosphate. Both the adsorbents showed the sharp peaks at 1,157.21 and 1,147.57 cm^{-1} as well as at 1,026.06 and 1,031.85 cm^{-1} which were assigned to –C–O vibration of polysaccharide and stretching vibration for bridge –C–O–C– of the glucosamine ring, respectively. Multiple bonded nitrogen compounds, such as diazo compounds, exhibit characteristic absorptions in the region 2,300–1,990 cm^{-1}.

Fig. 3[C](e) showed the IR spectrum of CR dye. The band at 1,614.31 cm^{-1} was attributed to –N=N– stretching vibration and bands in the 1,068.49, 1,180.35, and 1,221.71 cm^{-1}regions were attributed to S=O stretching vibrations. All the characteristic peaks

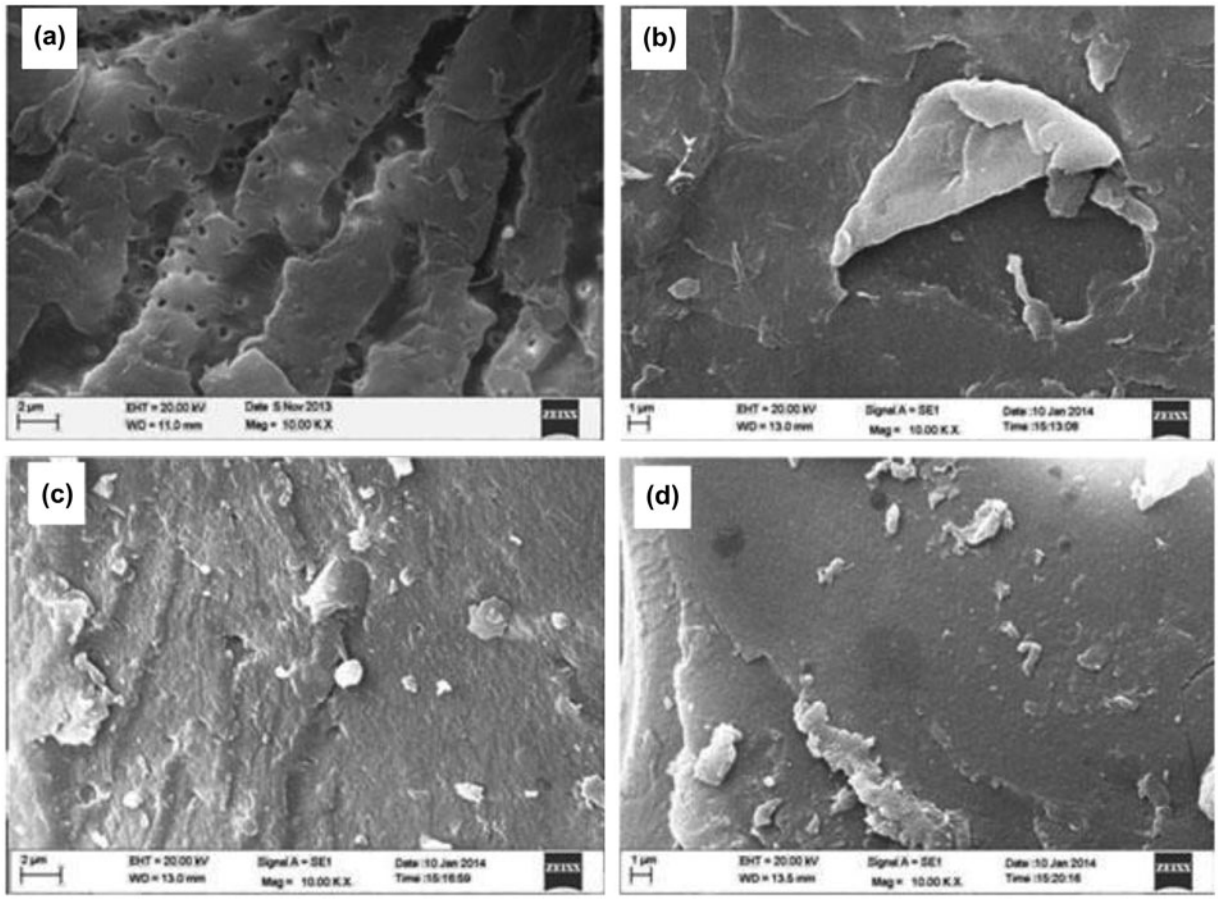

Fig. 2[A]. SEM images of CH beads before and after CR adsorption (a,b) and CTS beads before and after CR adsorption (c,d).

of CR are diminished after being adsorbed by adsorbents as observed in Fig. 3[A](b), Fig. 3[B](d).

From Fig. 3[A](b), Fig. 3[B](d), it can be clearly seen that the interactions occur between active sites present on both the adsorbents and SO_3 and –N=N– groups of CR, and thus all the characteristic peaks of both the adsorbents (–OH, $–NH_2$, and $–NHCOCH_3$ were diminished after adsorption of CR. Thus, it should be concluded that the adsorption of CR occurs by involving –OH, $–NH_2$, and $–NHCOCH_3$ groups present on adsorbents.

3.3. Effect of pH

The effect of pH ranging from 2.0 to 9.0 was investigated for the adsorption of CR, and the results were illustrated in Fig. 4. From the results, it was observed that initially when the pH value of the dye solution was raised from 2.0 to 7.0, the adsorption capacity reduced from 102.9 to 95.06 mg/g and from 103.53 to 97.02 mg/g for CH and CTS beads, respectively. Further increase in pH showed only slow reduction in adsorption capacity for both the adsorbents.

The possible mechanism of CR adsorption can be explicable as follows:

At lower pH, the electrostatic interaction between the protonated groups of both the adsorbents and the negatively charged dye anions causes an increase in dye adsorption. At pH value above 7.0, the excessive hydroxyl ions (OH^-) may compete with the dye anions for positively charged sites on the adsorbents and hence a slow reduction in dye uptake was observed. However, above pH 7.0 (at alkaline pH), there is still significant adsorption observed because of the chemical interaction between adsorbate and adsorbents.

As could be seen from Fig. 4, nearly the same adsorption capacity of CR on both the adsorbents could be found during highly acidic (2.0–5.0) and alkaline (≥9.0) pH values. However, CTS beads show

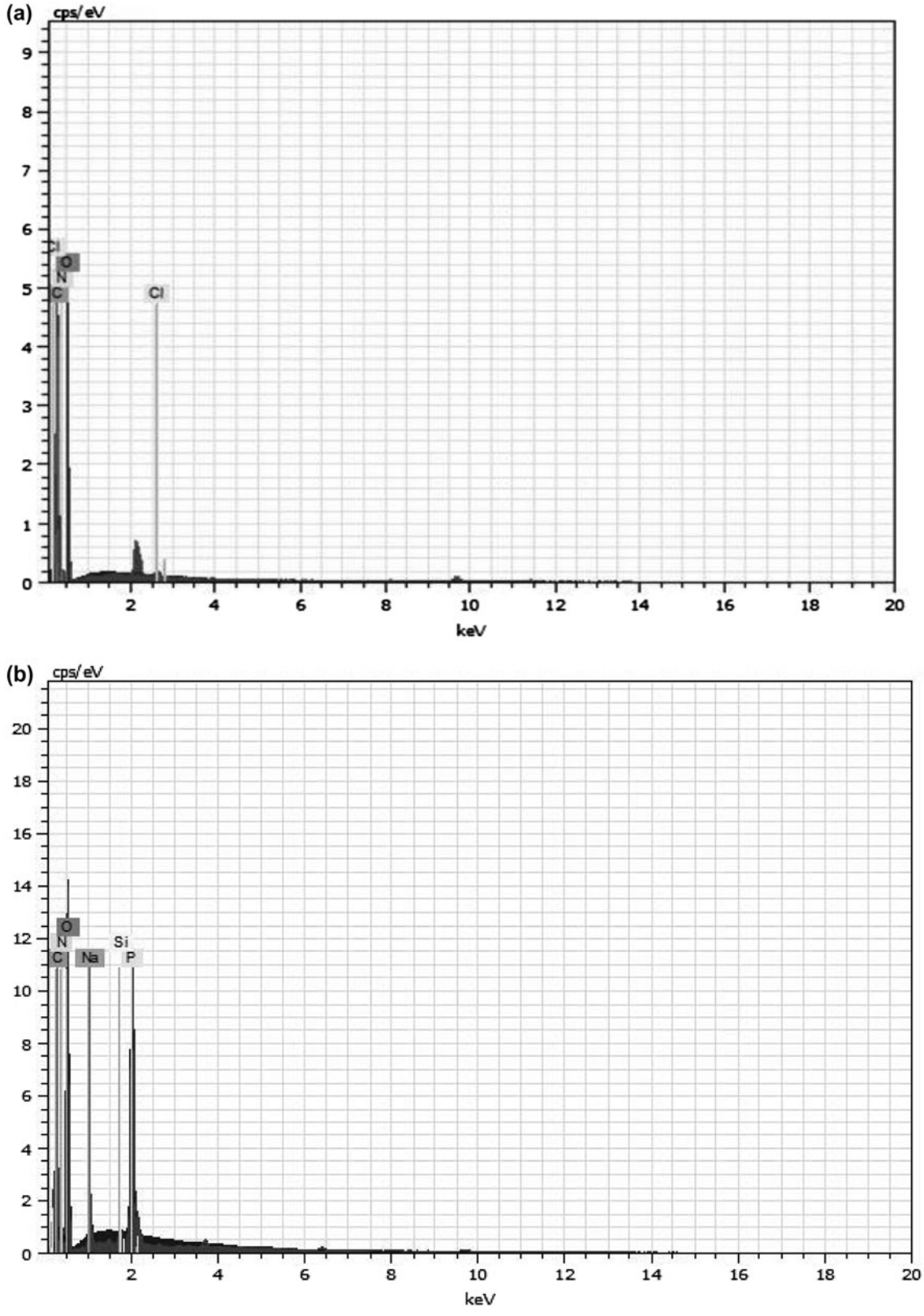

Fig. 2[B]. EDX spectra of CH (a) and CTS (b) beads.

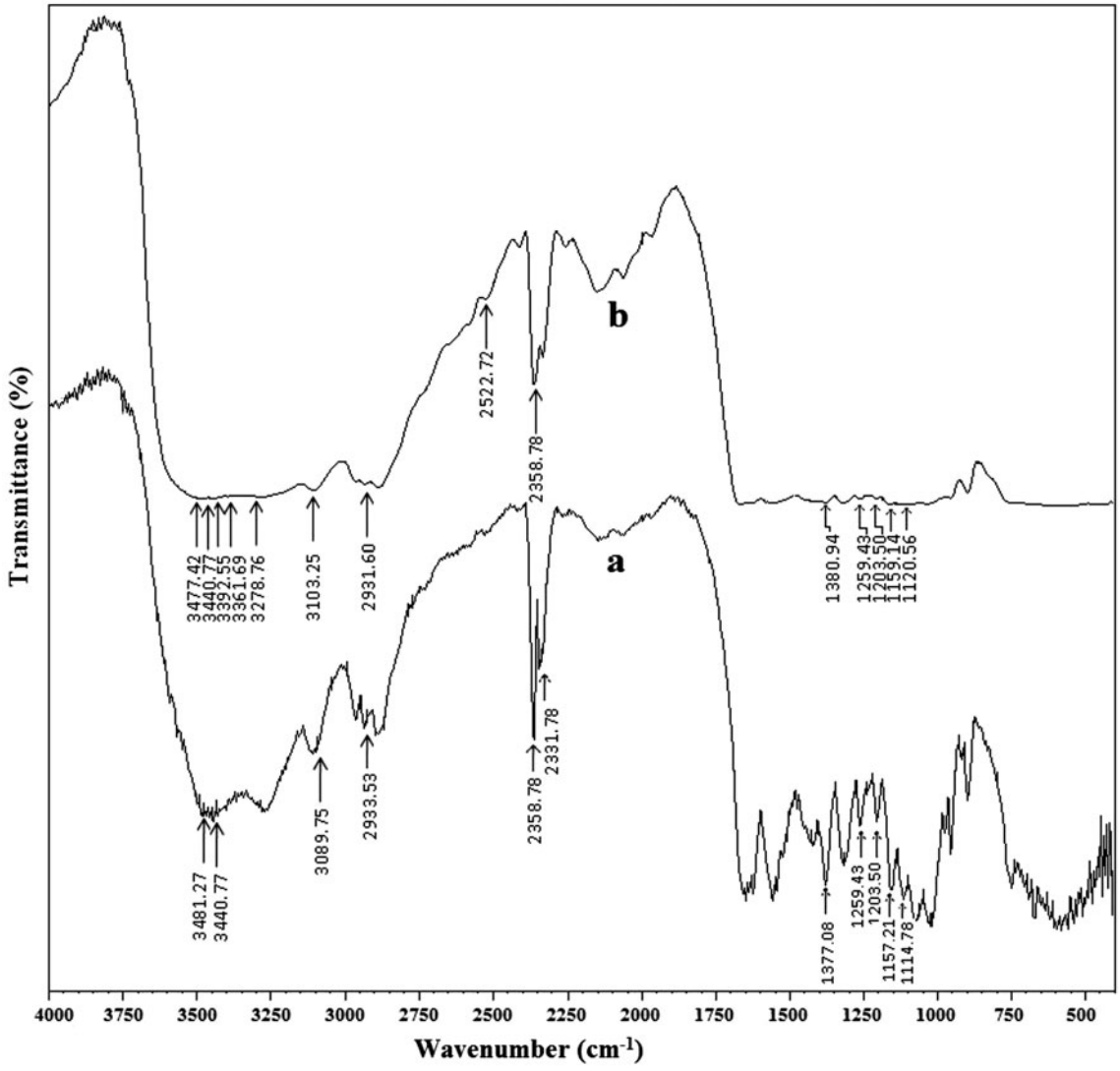

Fig. 3[A]. FT-IR spectra of CH beads (a); CR-loaded CH beads (b).

more adsorption capacity than CH beads between pH 6.0 and 8.0 because more active functional groups are available for CR adsorption on CTS beads. Thus, further studies were carried out at pH 6.0 for both the adsorbents.

3.4. Effect of initial dye concentration and contact time

The effects of initial dye concentration and contact time on the removal of CR by CH and CTS beads at the pH value of 6.0 are shown in Fig. 5. Four different concentrations, i.e. 35, 70, 105, and 140 mg/L, respectively, were selected to investigate the effect of initial dye concentration on the adsorption of CR onto adsorbents. From the same figure, it can be seen that with increasing initial dye concentration from 35 to 140 mg/L, the amount of dye adsorption was also increased from 34.02 to 106.47 mg/g and 34.496 to 129.22 mg/g for CH and CTS beads, respectively. The adsorption capacity increases with the increase in initial dye concentration due to a high driving force for mass transfer at enhanced dye concentration as well as the resistance to the uptake of CR from the solution decreased with the increase in CR concentration. When the surface active sites of adsorbents are covered fully, the extent of adsorption reaches a limit resulting in saturated adsorption.

Fig. 5 also represents the adsorption of dye as a function of contact time, varying from 1–120 min, for different initial dye concentrations. As the contact time

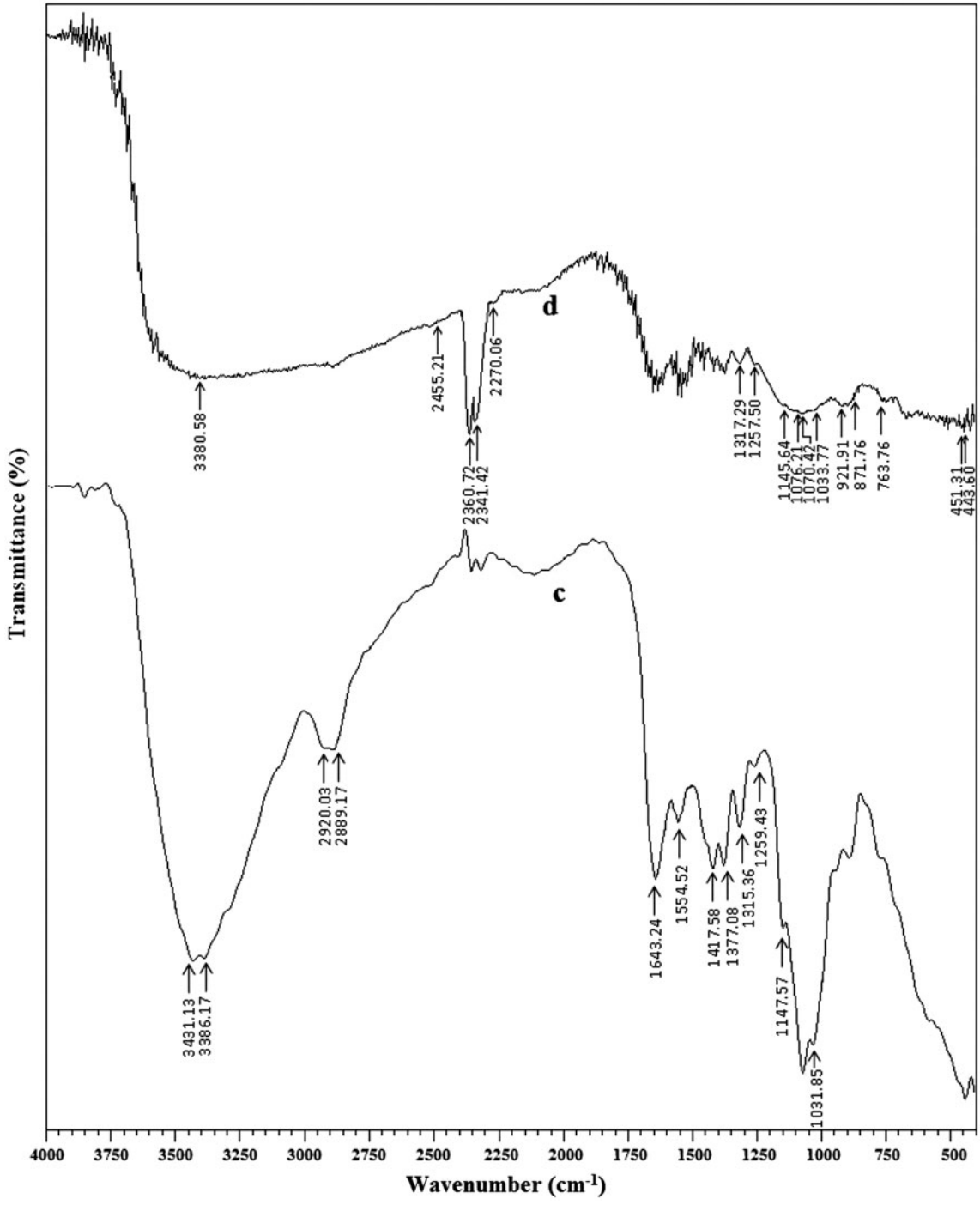

Fig. 3[B]. FT-IR Spectra of CTS beads (c); CR-loaded CTS beads (d).

increases, the adsorption of CR also increases, and equilibrium was achieved for both the adsorbents within 90 min. At maximum contact time, aggregation of dye molecules makes it almost impossible to diffuse deeper into the adsorbent structure at highest energy sites. Since the difference in the adsorption values at 90 min and at 120 min is very small, after 90 min contact, a steady-state approximation was achieved and a quasi-equilibrium situation was accepted. Based on the above results, 90 min contact time was fixed as equilibrium time throughout the adsorption study for both the adsorbents.

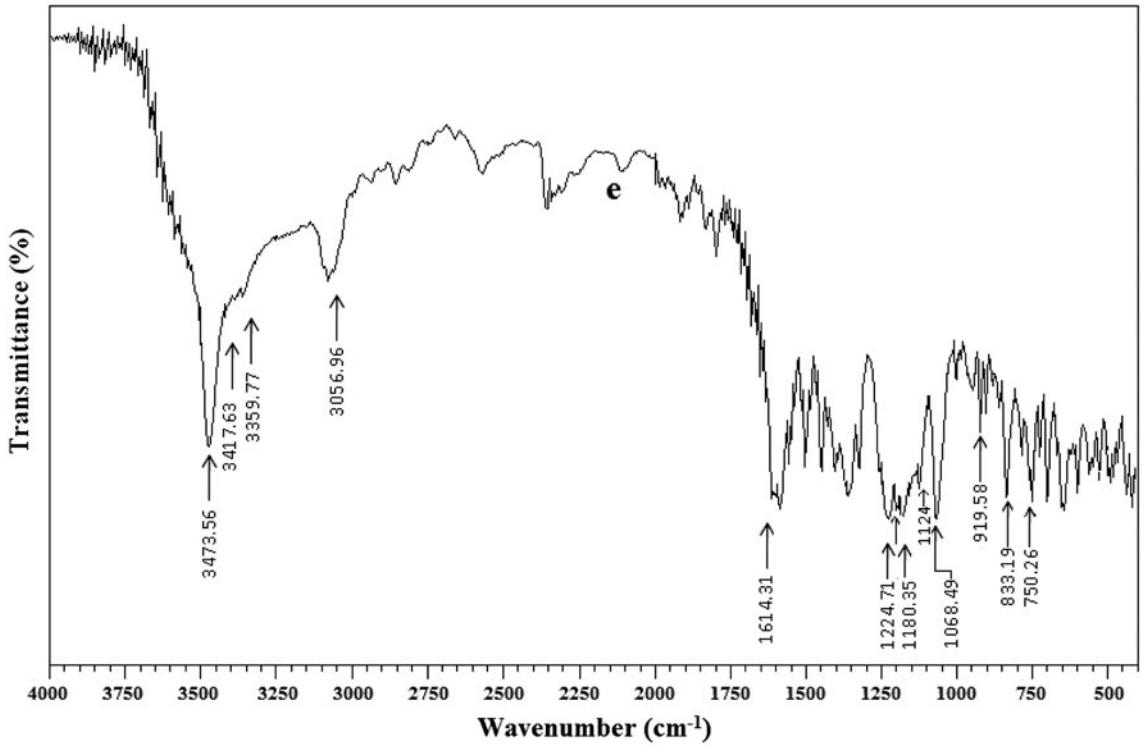

Fig. 3[C]. FT-IR Spectra of CR dye (e).

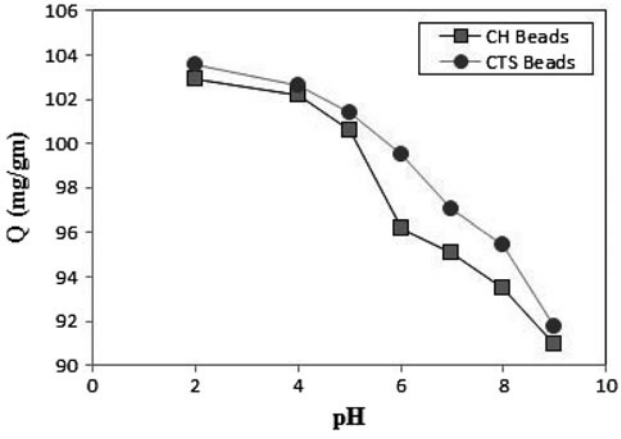

Fig. 4. Effects of pH on the adsorption of CR by CH and CTS beads [C_0=105 mg/L; contact time = 90 min; dosage of adsorbent = 100 mg; agitation speed = 120 rpm].

3.5. Effect of adsorbent dosage

The percentage of CR adsorption with varying amounts of CH and CTS beads is presented in Fig. 6(a). In general, the increase in adsorbent dosage (10 to 100 mg of adsorbent/100 mL of CR solution) increased the percent removal of adsorbate (from 39.53 to 95.8% and from 43.806 to 97.526% for CH and CTS beads, respectively). 100 mg adsorbent dosage was considered to be an optimum dosage as adsorption of CR almost remains constant. Initially, a rapid increase in adsorption with the increasing adsorbent dosage was attributed to availability of more adsorption sites [31]. The amount adsorbed (q_e) decreased from 415.1 to 100.59 mg/g and from 459.97 to 102.4 mg/g for both the adsorbents, respectively, when the adsorbents dosages was increased from 10 to 100 mg/100 mL (Fig. 6(b)). The decrease in amount of CR adsorbed onto adsorbents q_e (mg/g) with increasing adsorbents dosage is due to a split in the flux or the concentration gradient between CR concentration in the solution and the CR concentration on the surface of the adsorbents.

3.6. Equilibrium adsorption isotherms

Equilibrium adsorption isotherms describe the possible mechanism by which interaction occur between adsorbate and adsorbent. Therefore, the correlation of equilibrium data by either theoretical or empirical equations is important for predicting the adsorption capacity of the adsorbent [32]. The two most common models used to study adsorption isotherms are: (i) Langmuir Isotherm and (ii) Freundlich Isotherm.

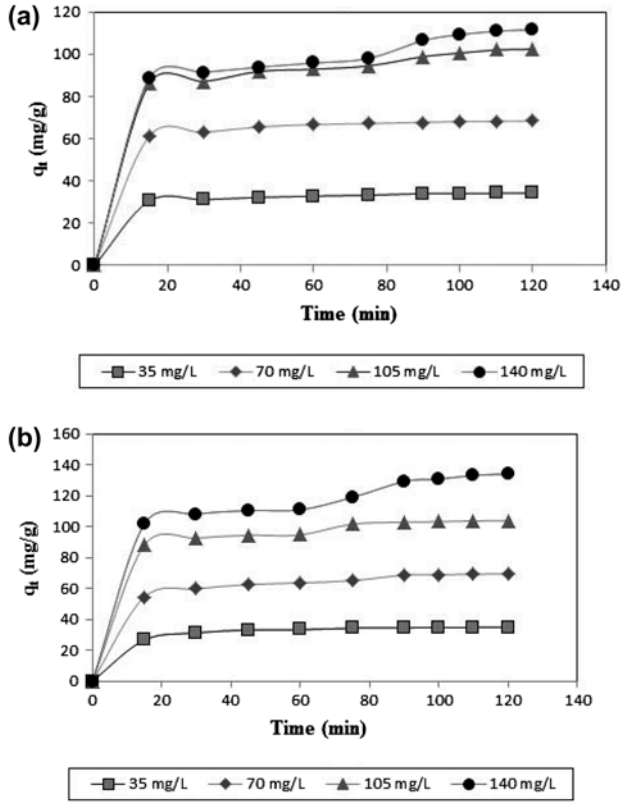

Fig. 5. Effects of initial dye concentrations and contact time on the adsorption of CR by CH (a) and CTS (b) Beads [pH 6.0; dosage of adsorbent = 100 mg; agitation speed = 120 rpm].

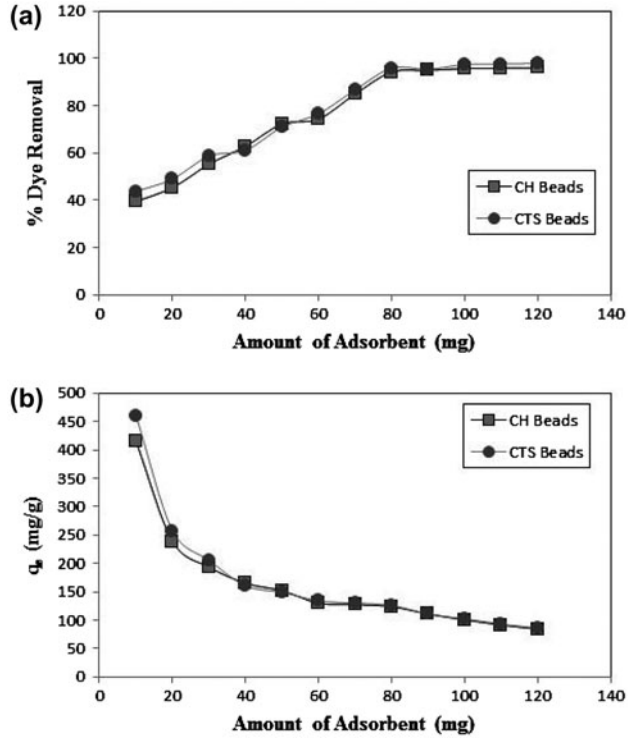

Fig. 6. Effects of amount of adsorbents on the percentage removal(**a**) and adsorption capacity (**b**) of CR by CH and CTS Beads [C_0=105 mg/L; pH 6.0; contact time = 90 min; agitation speed = 120 rpm].

Langmuir proposed a theory to describe the adsorption of gas molecules onto metal surfaces. The Langmuir adsorption isotherm has found successful applications in many other real adsorption processes of monolayer adsorption. The Langmuir model assumes that the each adsorbate molecule is located at specific homogenous sites within the adsorbent. Thus, it predicts the formation of a monolayer of the adsorbate on the homogenous adsorbent surface and does not consider surface heterogeneity of the adsorbent. The linear form of the Langmuir adsorption isotherm [33] is represented as:

$$\frac{C_e}{q_e} = \frac{1}{K_L} + \frac{a_L}{K_L} C_e \tag{3}$$

where C_e (in mg/L) is the equilibrium concentration of the CR in the solution. q_e (in mg/g) is the equilibrium adsorption capacity per gram dry weight of the adsorbent corresponding to complete coverage of the adsorptive sites. a_L (in L/mg) and K_L (in L/g) are the Langmuir isotherm constants. The values of a_L and K_L are calculated from the slope $\left(\frac{a_L}{K_L}\right)$ and intercept $\left(\frac{1}{K_L}\right)$ of the plot of $\frac{C_e}{q_e} \rightarrow C_e$. Ration of $\frac{K_L}{a_L}$ gives the value of monolayer sorption capacity of the adsorbent, q_m (in mg/g). Table 2 indicates that the maximum adsorption capacity of CH and CTS beads was 112.36 and 166.67 mg/g, respectively.

Table 2
Constants for equilibrium isotherm models with error analysis values for CH and CTS beads

Adsorbents	K_L (L/g)	q_m (mg/g)	R_L^*	R^2	χ^2
Langmuir Isotherm					
Chitin	72.464	112.36	0.0109	0.998	3.518
Chitosan	111.111	166.67	0.0106	0.995	2.714
Adsorbents	K_F (L/g)	$1/n$	n	R^2	χ^2
Freundlich Isotherm					
Chitin	44.361	0.298	3.356	0.758	13.755
Chitosan	43.652	0.458	2.183	0.949	20.584

*C_0=140 mg/L.

The essential characteristic feature of Langmuir isotherm can be expressed in terms of "R_L", a dimensionless constant referred to as "separation factor" or "equilibrium parameter". The value of R_L is calculated using the following equation:

$$R_L = \frac{1}{(1 + a_L\ C_0)} \tag{4}$$

The R_L value indicates whether the adsorption is unfavorable ($R_L > 1$), linear ($R_L = 1$), favorable ($0 < R_L < 1$), or irreversible ($R_L = 0$) [34,35]. R_L values of CH beads (0.0109) and CTS beads (0.0106) for the initial CR concentration of 140 mg/L indicate favorable adsorption of CR onto both CH and CTS beads.

Freundlich adsorption isotherm defines the adsorption onto the adsorbent with heterogeneous surface. The linear form of Freundlich isotherm model [36] is as follows:

$$\log q_e = \log K_F + \frac{1}{n} \log C_e \tag{5}$$

where K_F (in L/g) is the Freundlich adsorption isotherm constant, relating to the extent of adsorption. n (in g/L) is the Freundlich exponent. The values of K_F and $\frac{1}{n}$ are calculated from the slope and intercept of the plot of $\log q_e \rightarrow \log C_e$ and are listed in Table 2.

Fig. 7 shows the equilibrium adsorption of CR using CH (a) and CTS (b) beads (q_e vs. C_e), and the isotherms are plotted together with the experimental data points. For both the adsorbents, Langmuir isotherm model shows good fit to experimental data.

3.7. Error analysis

In the single component isotherm studies, the optimization procedure requires an error function to be defined in order to be able to evaluate the fit of the isotherm equation to the experimental equilibrium data. In this study, linear coefficient of determination (R^2) and a non-linear Chi-square test (χ^2) were performed for both the isotherms.

The Chi-square test statistics is basically the sum of the squares of the differences between the experimental data and the data obtained by calculating from models, with each squared difference divided by the corresponding data obtained by calculating from models. The mathematical equation can be represented as:

$$\chi^2 = \sum \frac{(q_{e(\exp)} - q_{e(\text{cal})})^2}{q_{e(\text{cal})}} \tag{6}$$

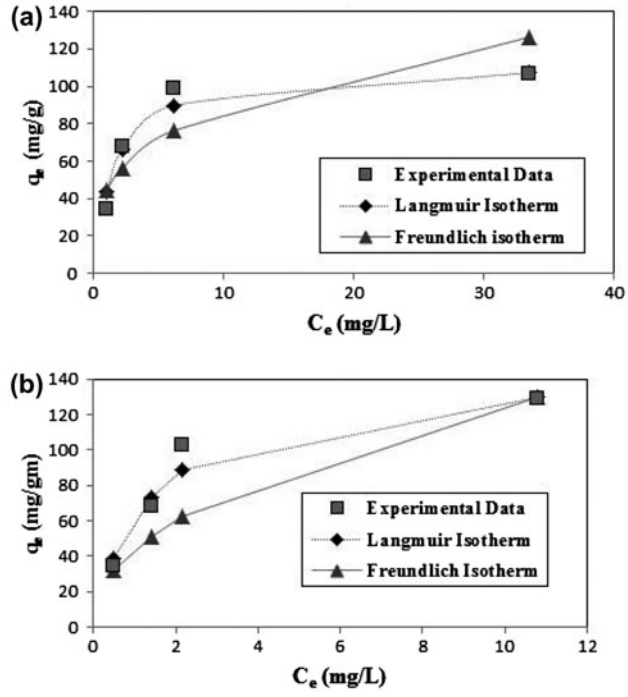

Fig. 7. Plot of qe vs. Ce for the adsorption of CR onto CH (a) and CTS (b) Beads [pH 6.0; contact time = 90 min; dosage of adsorbent = 100 mg/100 mL; agitation speed = 120 rpm].

where $q_{e(\exp)}$(in mg/g) is the experimental data of the equilibrium capacity; $q_{e(\text{cal})}$ (in mg/g) is the equilibrium capacity obtained by calculating from the model. If data from the model are similar to the experimental data, χ^2 will be a smaller number, and if they differ, χ^2 will be a bigger number. Therefore, it is necessary to analyze the data using the non-linear Chi-square test to confirm the best fit isotherm for this adsorption system [37,38].

The results of the linear coefficient of determination (R^2) and a non-linear Chi-square test (χ^2) for two adsorption isotherms indicated that the Langmuir isotherm model appeared to be the best fitting model for adsorption of CR onto CH and CTS beads.

3.8. Adsorption kinetics

Study of sorption kinetics provides valuable insights into the reaction pathways and in turn controls the residence time of adsorbate uptake at the solid–solution interface. In addition, kinetics study is helpful for selecting optimum operating conditions for the full-scale batch process [39]. In this study, to investigate the adsorption of CR onto CH and CTS beads, two different rate models (pseudo-first-order and pseudo-second-order) were used.

Table 3
Kinetic parameters for the removal of CR by both the adsorbents

Adsorbents			Chitin			Chitosan		
Pseudo-first-order constants	C_0 (mg/L)	$q_{e(exp)}$ (mg/g)	$q_{e(cal)}$ (mg/g)	k_1 (min^{-1})	R^2	$q_{e(cal)}$ (mg/g)	k_1 (min^{-1})	R^2
	35	34.02	5.6754	0.025333	0.986	18.03	0.052969	0.937
	70	67.76	14.421	0.041454	0.986	18.3231	0.02303	0.982
	105	98.84	17.989	0.018424	0.96	32.1366	0.034545	0.714
	140	106.47	21.727	0.011515	0.996	34.435	0.013818	0.856
Pseudo-second-order constants	C_0 (mg/L)	$q_{e(exp)}$ (mg/g)	$q_{e(cal)}$ (mg/g)	k_2 (g/mg min)	R^2	$q_{e(cal)}$ (mg/g)	k_2 (g/mg min)	R^2
	35	34.02	34.483	0.0123	0.999	33.33	0.0060	1
	70	67.76	69.44	0.00591	0.999	66.67	0.00375	1
	105	98.84	100	0.0037	0.999	100	0.0025	1
	140	106.47	111.111	0.00312	0.999	125	0.0020	0.996

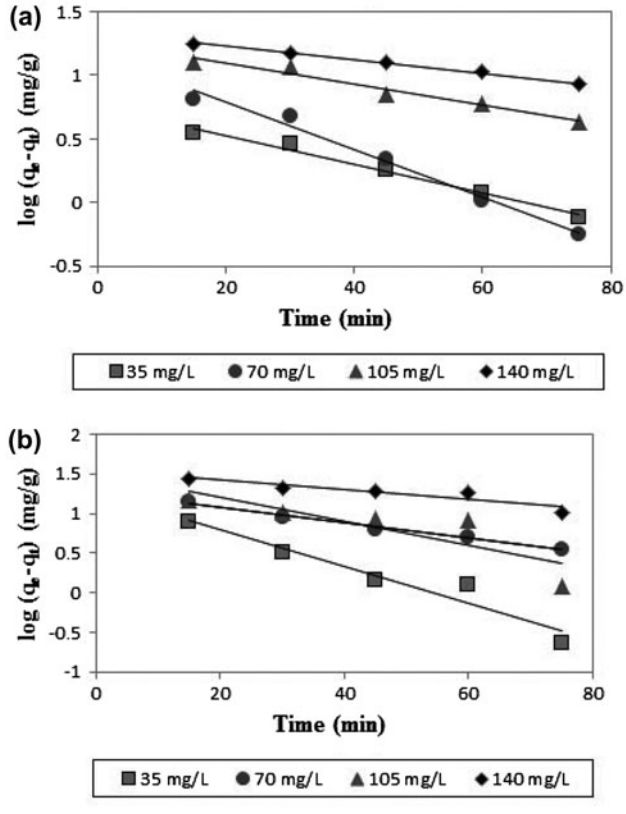

Fig. 8. Pseudo-first-order model for the adsorption of CR onto CH (a) and CTS (b) Beads [pH 6.0; dosage of adsorbent = 100 mg/100 mL; agitation speed = 120 rpm].

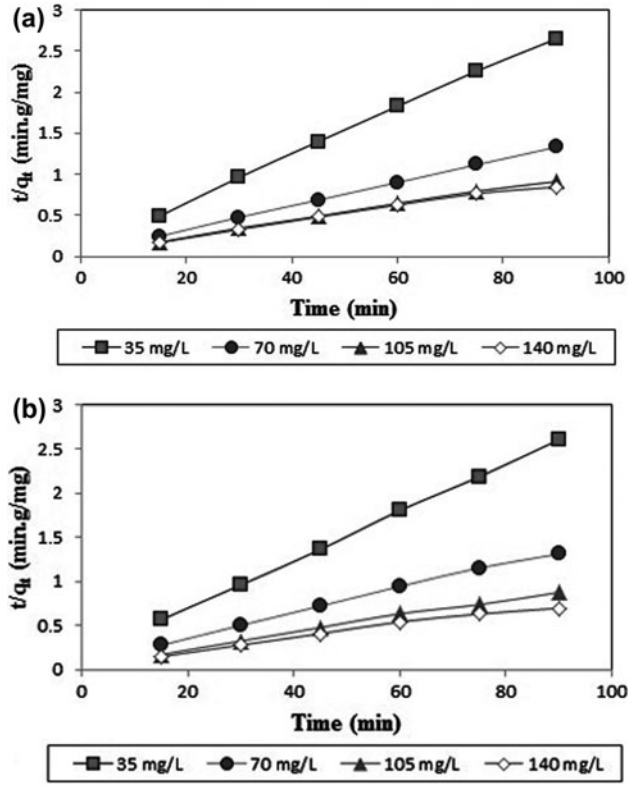

Fig. 9. Pseudo-second-order model for the adsorption of CR onto CH (a) and CTS (b) Beads [pH 6.0; dosage of adsorbent = 100 mg/100 mL; agitation speed = 120 rpm].

Table 4
Comparison between adsorption capacities of various adsorbents

Sr. No.	Adsorbent	q_{max} (mg/g)	References
1	Activated carbon—commercial grade	0.64	[8]
2	Paddy straw	1.01	[42]
3	Activated carbon—laboratory grade	1.88	[8]
4	Waste red mud	4.05	[43]
5	Kaolin	5.44	[44]
6	Coconut coir pith	6.72	[45]
7	Activated red mud	7.08	[46]
8	$NaHCO_3$ pretreated *Aspergillus niger* biomass	8.19	[47]
9	Biogas waste slurry	9.50	[48]
10	Bagasse fly ash	11.89	[8]
11	Waste banana pith	20.29	[49]
12	Orange peel	22.44	[50]
13	Neem leaf powder	41.20	[9]
14	Waste Fe(III)/Cr(III) hydroxide	44.00	[51]
15	CTS-MMT	54.52	[52]
16	CTS Powder	74.73	[52]
17	Chitosan hydrobeads	93.71	[54]
18	N,O-Carboxymethyl chitosan	330.62	[53]
19	CS/CTAB beads	385.90	[18]
20	CS/CNT beads	450.40	[10]
21	Chitin (CH) beads	112.36	This Work
22	Chitosan–tripolyphosphate (CTS) beads	166.67	This Work

A pseudo-first-order kinetic model of Lagergren [40] is given as:

$$\log\,(q_e - q_t) = \log\, q_e - \frac{k_1}{2.303}\, t \tag{7}$$

where q_e (in mg/g) and q_t (in mg/g) are the amounts of dye adsorbed on adsorbent at equilibrium and at time t, respectively, and k_1 (m^{-1}) is the pseudo-first-order rate constant.

The linearized pseudo-second-order kinetic equation [41] is given as:

$$\frac{t}{q_t} = \frac{1}{k_2 q_e^2} + \frac{t}{q_e} \tag{8}$$

where k_2 (in g/mg m) is the pseudo-second-order rate constant. The values of k_2 and q_e for pseudo-second-order rate model are calculated from intercept and slope of the $\frac{t}{q_t}$ vs. t plots and given in Table 3.

It can be seen that the values of the correlation coefficient for both the pseudo-first-order and pseudo-second-order rate models were closer to unity. However, the pseudo-second-order model described very well the adsorption of CR onto CH and CTS beads because the experimental q_e values are very close to the calculated q_e values for pseudo-second-order rate model. As shown in table, the values of the rate constant k_2 decreases with increasing initial CR dye concentration because higher dye concentration corresponds to higher surface loading which decreases the diffusion efficiency. The plots of pseudo-first-order and pseudo-second-order models were shown in Figs. 8 and 9.

3.9. Performance evaluation

The maximum adsorption capacities (q_{max}) of CH and CTS beads calculated from the Langmuir isotherm model for CR adsorption, in comparison with the literature values of q_{max} of other adsorbents, are listed in Table 4. All the adsorbents used for CR adsorption have lower q_{max} values than the adsorbents used in this study. Some chemically modified adsorbents such as, N,O—Carboxymethyl CTS, CS/CTAB beads, and CS/CNT beads have higher CR adsorption capacity, but they generally require other chemical grafting reactions as well as addition of surfactants which ultimately adversely affects the environment. On the other hand, CH and CTS are easily available which can be used without grafting with harsh chemicals, their utilization as adsorbents for removal of dye is expected to be economical.

4. Conclusions

The present investigations show that CH and CTS beads can be effectively used and compared as an adsorbent for the removal of hazardous anionic azo dye CR from wastewater. Both the adsorbents were characterized by SEM, EDX, and FT-IR, and the results confirm the heterogeneous and porous structure of the beads as well as the presence of main functional groups such as –OH, $–NH_2$, and $–NHCOCH_3$. For both the adsorbents, effects of the parameters like pH, adsorbate concentration, contact time, and dosage of adsorbents on adsorption of CR were investigated. From the analysis, it was observed that the amount of CR adsorbed on both the adsorbents increases with increasing initial dye concentration and decreasing pH. The equilibrium contact time and dosage of adsorbents were 90 min and 100 mg/100 mL, respectively, for both the adsorbents. The adsorption process followed well to the Langmuir adsorption isotherm and the maximum adsorption capacities were 112.36 and 166.67 mg/g for CH and CTS beads, respectively. Further, the pseudo-first-order and second-order kinetic models were used to describe the kinetic data, and the rate constants were evaluated. The dynamical data fit well with the second-order kinetic model.

Acknowledgments

The authors express their sincere gratitude to INSPIRE Programme of Department of Science and Technology (DST) for the financial support of this study. This research was supported by INSPIRE programme under the Assured Opportunity for Research Careers (AORC), funded by the Department of Science and Technology (DST) (Sanction Order No.: DST/INSPIRE Fellowship/2013/66).

Abbreviations

CH beads	—	chitin beads
CTS beads	—	chitosan–tripolyphosphate beads
CR	—	Congo Red
SEM	—	scanning electron microscopy
FT–IR	—	Fourier transform infrared spectroscopy
UV–Vis.	—	ultraviolet–visible spectrophotometer

List of Symbols

$R\%$	—	removal percentage of dye
q_e	—	the equilibrium adsorption capacity per gram (dry weight) of the adsorbent (mg/g)
C_0	—	the initial concentration of CR in the solution (mg/L)
C_e	—	the equilibrium concentration of CR in the solution (mg/L)
V	—	the volume of the solution (mL)
W	—	the dry weight of CH and CTS beads (mg)
a_L	—	the Langmuir isotherm constant (L/mg)
K_L	—	the Langmuir isotherm constant (L/g)
q_m	—	the monolayer sorption capacity of the adsorbent (mg/g)
R^2	—	the linear coefficient of determination
R_L	—	separation factor or equilibrium parameter (Dimensionless)
K_F	—	the Freundlich adsorption isotherm constant (L/g)
n	—	the Freundlich exponent (g/L)
χ^2	—	a non-linear Chi-square test
$q_{e(\exp)}$	—	the experimental data of the equilibrium capacity (mg/g)
$q_{e(\mathrm{cal})}$	—	the equilibrium capacity obtained by calculating from the model(mg/g)
T	—	time (min)
q_t	—	the amounts of dye adsorbed on adsorbent at time t (mg/g)
k_1	—	the pseudo-first-order rate constant (m^{-1})
k_2	—	the pseudo-second-order rate constant (g/mg min)

References

[1] M. Solís, A. Solís, H.I. Pérez, N. Manjarrez, M. Flores, Microbial decolouration of azo dyes: A review, Process Biochem. 47(12) (2012) 1723–1748.
[2] R. Sivaraj, C. Namasivayam, K. Kadirvelu, Orange peel as an adsorbent in the removal of Acid violet 17 (acid dye) from aqueous solutions, Waste Manage. 21 (1) (2001) 105–110.
[3] H. Zhu, R. Jiang, L. Xiao, Y. Chang, Y. Guan, X. Li, G. Zeng, Photocatalytic decolorization and degradation of congo red on innovative crosslinked chitosan/nano-CdS composite catalyst under visible light irradiation, J. Hazard. Mater. 169(1–3) (2009) 933–940.
[4] M. Unlu, H. Yukseler, U. Yetis, Indigo dyeing wastewater reclamation by membrane-based filtration and coagulation processes, Desalination 240(1–3) (2009) 178–185.
[5] K. Selvam, K. Swaminathan, K. Chae, Decolourization of azo dyes and a dye industry effluent by a white rot fungus *Thelephora* sp., Bioresour. Technol. 88(2) (2003) 115–119.
[6] N. Puvaneswari, J. Muthukrishnan, P. Gunasekaran, Toxicity assessment and microbial degradation of azo dyes, Indian J. Exp. Biol. 44(8) (2006) 618–626.
[7] R. Han, D. Ding, Y. Xu, W. Zou, Y. Wang, Y. Li, L. Zou, Use of rice husk for the adsorption of congo red from aqueous solution in column mode, Bioresour. Technol. 99(8) (2008) 2938–2946.

[8] I. Mall, V. Srivastava, N. Agarwal, I. Mishra, Removal of congo red from aqueous solution by bagasse fly ash and activated carbon: Kinetic study and equilibrium isotherm analyses, Chemosphere 61(4) (2005) 492–501.
[9] K. Bhattacharyya, A. Sharma, *Azadirachta indica* leaf powder as an effective biosorbent for dyes: A case study with aqueous congo red solutions, J. Environ. Manage. 71(3) (2004) 217–229.
[10] S. Chatterjee, M.W. Lee, S.H. Woo, Adsorption of congo red by chitosan hydrogel beads impregnated with carbon nanotubes, Bioresour. Technol. 101(6) (2010) 1800–1806.
[11] S. Sadri Moghaddam, M.R. Alavi Moghaddam, M. Arami, Coagulation/flocculation process for dye removal using sludge from water treatment plant: Optimization through response surface methodology, J. Hazard. Mater. 175(1–3) (2010) 651–657.
[12] M.S. Lucas, J.A. Peres, Decolorization of the azo dye Reactive Black 5 by Fenton and photo-Fenton oxidation, Dyes Pigm. 71(3) (2006) 236–244.
[13] F. Zhang, A. Yediler, X. Liang, A. Kettrup, Effects of dye additives on the ozonation process and oxidation by products: A comparative study using hydrolyzed C.I. Reactive Red 120, Dyes Pigm. 60(1) (2004) 1–7.
[14] N. Al-Bastaki, Removal of methyl orange dye and Na_2SO_4 salt from synthetic waste water using reverse osmosis, Chem. Eng. Process. 43(12) (2004) 1561–1567.
[15] S. Sachdeva, A. Kumar, Preparation of nanoporous composite carbon membrane for separation of rhodamine B dye, J. Membr. Sci. 329(1–2) (2009) 2–10.
[16] A. Alinsafi, M. Khemis, M.N. Pons, J.P. Leclerc, A. Yaacoubi, A. Benhammou, A. Nejmeddine, Electrocoagulation of reactive textile dyes and textile wastewater, Chem. Eng. Process. 44(4) (2005) 461–470.
[17] K. Gopinath, S. Murugesan, J. Abraham, K. Muthukumar, *Bacillus* sp. mutant for improved biodegradation of congo red: Random mutagenesis approach, Bioresour. Technol. 100(24) (2009) 6295–6300.
[18] S. Chatterjee, D.S. Lee, M.W. Lee, S.H. Woo, Enhanced adsorption of congo red from aqueous solutions by chitosan hydrogel beads impregnated with cetyl trimethyl ammonium bromide, Bioresour. Technol. 100 (11) (2009) 2803–2809.
[19] Z. Aksu, Application of biosorption for the removal of organic pollutants: A review, Process Biochem. 40(3–4) (2005) 997–1026.
[20] T. Kurniawan, G. Chan, W.H. Lo, S. Babel, Physicochemical treatment techniques for wastewater laden with heavy metals, Chem. Eng. J. 118(1–2) (2006) 83–98.
[21] A. Gamage, F. Shahidi, Use of chitosan for the removal of metal ion contaminants and proteins from water, Food Chem. 104(3) (2007) 989–996.
[22] N.V. Manjeti, R. Kumar, A review of chitin and chitosan applications, React. Funct. Polym. 46(1) (2000) 1–27.
[23] K. Azlan, W.N. Wan Saime, L. Lai Ken, Chitosan and chemically modified chitosan beads for acid dyes sorption, J. Environ. Sci. 21(3) (2009) 296–302.
[24] A. Kamari, W. Ngah, M. Chong, M. Cheah, Sorption of acid dyes onto GLA and H_2SO_4 cross-linked chitosan beads, Desalination 249(3) (2009) 1180–1189.
[25] S. Chatterjee, T. Chatterjee, S.R. Lim, S.H. Woo, Adsorption of a cationic dye, methylene blue, on to chitosan hydrogel beads generated by anionic surfactant gelation, Environ. Technol. 32(13) (2011) 1503–1514.
[26] M.S. Chiou, W.S. Kuo, H.Y. Li, Removal of reactive dye from wastewater by adsorption using ECH crosslinked chitosan beads as medium, J. Environ. Sci. Health A Tox. Hazard. Subst. Environ. Eng. 38(11) (2003) 2621–2631.
[27] M.S. Chiou, H.Y. Li, Equilibrium and kinetic modeling of adsorption of reactive dye on cross-linked chitosan beads, J. Hazard. Mater. 93(2) (2002) 233–248.
[28] M. Vakili, M. Rafatullah, B. Salamatinia, A.Z. Abdullah, M.H. Ibrahim, K.B. Tan, Z. Gholami, P. Amouzgar, Application of chitosan and its derivatives as adsorbents for dye removal from water and wastewater: A review, Carbohydr. Polym. 113 (2014) 115–130.
[29] E. Yilmaz, M. Bengisu, Preparation and characterization of physical gels and beads from chitin solutions, Carbohydr. Polym. 54(4) (2003) 479–488.
[30] R. Laus, V. de Fávere, Competitive adsorption of Cu(II) and Cd(II) ions by chitosan crosslinked with epichlorohydrin–triphosphate, Bioresour. Technol. 102 (19) (2011) 8769–8776.
[31] K. Deepa, M. Sathishkumar, A. Binupriya, G. Murugesan, K. Swaminathan, S. Yun, Sorption of Cr(VI) from dilute solutions and wastewater by live and pretreated biomass of *Aspergillus flavus*, Chemosphere 62(5) (2006) 833–840.
[32] Y. Wong, Y. Szeto, W. Cheung, G. McKay, Adsorption of acid dyes on chitosan-equilibrium isotherm analyses, Process Biochem. 39(6) (2004) 695–704.
[33] I. Langmuir, The adsorption of gases on plane surfaces of glass, mica and platinum, J. Am. Chem. Soc. 40(9) (1918) 1361–1403.
[34] W. Nagh, C. Endud, R. Mayanar, Removal of copper (II) ions from aqueous solution onto chitosan and cross-linked chitosan beads, React. Funct. Polym. 50(2) (2002) 181–190.
[35] C. Futalan, C. Kan, M. Dalida, K. Hsien, C. Pascua, M. Wan, Comparative and competitive adsorption of copper, lead, and nickel using chitosan immobilized on bentonite, Carbohydr. Polym. 83(2) (2011) 528–536.
[36] H.M.F. Freundlich, Über die adsorption in lösungen (Over the adsorption in solution), J. Phys. Chem. 57 (1906) 385–470 (in German).
[37] E. Unuabonah, B. Olu-Owolabi, K. Adebowale, A. Ofomaja, Adsorption of lead and cadmium ions from aqueous solutions by tripolyphosphate-impregnated Kaolinite clay, Colloids Surf., A 292(2–3) (2007) 202–211.
[38] Y. Ho, W. Chiu, C. Wang, Regression analysis for the sorption isotherms of basic dyes on sugarcane dust, Bioresour. Technol. 96(11) (2005) 1285–1291.
[39] M. Kalavathy, T. Karthikeyan, S. Rajgopal, L. Miranda, Kinetic and isotherm studies of Cu(II) adsorption onto H3PO4-activated rubber wood sawdust, J. Colloid Interface Sci. 292(2) (2005) 354–362.
[40] S. Lagergren, Zur Theorie der Soge-Nannten Adsorption Gel?ster Stoffe (About the theory of so-called adsorption of soluble substances), K. Sven. Vetenskapsakad. Handl. Band 24(4) (1898) 1–39.
[41] Y. Ho, G. McKay, Pseudo-second order model for sorption processes, Process Biochem. 34(5) (1999) 451–465.

[42] N. Deo, M. Ali, Dye adsorption by a new low cost material: Congo red-1, Indian J. Environ. Prot. 13 (1993) 496–508.
[43] C. Namasivayam, D. Arasi, Removal of congo red from wastewater by adsorption onto waste red mud, Chemosphere 34(2) (1997) 401–417.
[44] V. Vimonses, S. Lei, B. Jin, C. Chow, C. Saint, Kinetic study and equilibrium isotherm analysis of congo red adsorption by clay materials, Chem. Eng. J. 148(2–3) (2009) 354–364.
[45] C. Namasivayam, D. Kavitha, Removal of congo red from water by adsorption onto activated carbon prepared from coir pith, an agricultural solid waste, Dyes Pigm. 54(1) (2002) 47–58.
[46] A. Tor, Y. Cengeloglu, Removal of congo red from aqueous solution by adsorption onto acid activated red mud, J. Hazard. Mater. 138(2) (2006) 409–415.
[47] Y. Fu, T. Viraraghavan, Removal of congo red from an aqueous solution by fungus *Aspergillus niger*, Adv. Environ. Res. 7(1) (2002) 239–247.
[48] C. Namasivayam, R.T. Yamuna, Removal of congo red from aqueous solution by biogas waste slurry, J. Chem. Technol. Biotechnol. 53(2) (1992) 153–157.
[49] C. Namasivayam, N. Kanchana, Waste banana pith as adsorbent for color removal from wastewaters, Chemosphere 25(11) (1992) 1691–1705.
[50] C. Namasivayam, N. Muniasamy, K. Gayatri, M. Rani, K. Ranganathan, Removal of dyes from aqueous solutions by cellulosic waste orange peel, Bioresour. Technol. 57(1) (1996) 37–43.
[51] C. Namasivayam, R. Jeyakumar, R.T. Yamuna, Dye removal from wastewater by adsorption on 'waste' Fe(III)/Cr(III) hydroxide, Waste manage. 14(7) (1994) 643–648.
[52] L. Wang, A. Wang, Adsorption characteristics of congo red onto the chitosan/montmorillonite nanocomposite, J. Hazard. Mater. 147(3) (2007) 979–985.
[53] L. Wang, A. Wang, Adsorption behaviors of congo red on the N, O-carboxymethyl-chitosan/montmorillonite nanocomposite, Chem. Eng. J. 143(1–3) (2008) 43–50.
[54] S. Chatterjee, S. Chatterjee, B. Chatterjee, A. Guha, Adsorptive removal of congo red, a carcinogenic textile dye by chitosan hydrobeads: Binding mechanism, equilibrium and kinetics, Colloids Surf., A 299(1–3) (2007) 146–152.